Water Research 211 (2022) 118041

Contents lists available at ScienceDirect

Water Research

journal homepage: www.elsevier.com/locate/watres

Insight into phototransformation mechanism and toxicity evolution of novel and legacy brominated flame retardants in water: A comparative analysis

Ya Cao [a,c], Yanpeng Gao [b,*], Xinyi Hu [b], Yanhong Zeng [a], Xiaojun Luo [a], Guiying Li [b], Taicheng An [b], Bixian Mai [a]

[a] State Key Laboratory of Organic Geochemistry and Guangdong Key Laboratory of Environmental Protection and Resources Utilization, Guangzhou Institute of Geochemistry, Chinese Academy of Sciences, Guangzhou 510640, China
[b] Guangdong-Hong Kong-Macao Joint Laboratory for Contaminants Exposure and Health, Guangdong Key Laboratory of Environmental Science and Engineering, Institute of Environmental Health and Pollution Control, Guangdong University of Technology, Guangzhou 510006, China
[c] University of Chinese Academy of Sciences, Beijing 100049, China

ARTICLE INFO

Keywords:
BTBPE
Novel brominated flame retardants
Phototransformation
Compound-specific isotope analysis
Degradation mechanism

ABSTRACT

The novel brominated flame retardants (NBFRs) have become widespread as a consequence of the prohibition on the use of polybrominated diphenyl ethers (PBDEs). However, the transformation mechanism and potential environmental risk are largely unclear. In this study, we have explored the phototransformation behavior of the most abundant NBFRs, 1,2-bis(2,4,6-tribromophenoxy)ethane (BTBPE) in water under ultraviolet (UV) irradiation. Meanwhile, the legacy 2,2′,4,4′,6,6′-hexabromodiphenyl ether (BDE155) with similar structure was investigated contrastively. Results show that novel BTBPE is more persistent than legacy BDE155, with nearly four times slower photodegradation rate constants (0.0120 $min^{-1}$and 0.0447 min^{-1}, respectively). 18 products are identified in the phototransformation of BTBPE. Different from the only debrominated products formed in legacy BDE155 transformation, the ether bond cleavage photoproducts (e.g. bromophenols) are also identified in novel BTBPE transformation. Compound-specific stable isotope analysis (CSIA) confirms the phototransformation mechanism is mainly via debromination accompanying with the breaking of ether bond. Computational toxicity assessment implies that transformation products of BTBPE still have the high kidney risks. Especially the bromophenols formed via the ether bond cleavage could significantly increase the health effects on skin irritation. This study emphasizes the importance of understanding the photolytic behavior and potential risks of novel NBFRs and other structurally similar analogues.

1. Introduction

Brominated flame retardants (BFRs) have caused a global environmental concern for several decades due to its serious harm to environment and human health. In particular, polybrominated diphenyl ethers (PBDEs) have been prohibited or restricted in many countries (Renner, 2004; Tang, 2013). Accordingly, as the important replacement of these banned BFRs, several novel brominated flame retardants (NBFRs) are emerging into market. Particularly, 1,2-Bis(2,4,6-tribromophenoxy) ethane (BTBPE) is one of the most deployed NBFRs in recent years. Given the huge production and wide application for several decades, NBFRs have been frequently detected in various environmental matrices, including water (Wang et al., 2020; Zhang et al., 2015), air (Ma et al., 2012), sediment (Kolic et al., 2009; Shi et al., 2009), biota samples (Verreault et al., 2007; Wu et al., 2020), foods (Li et al., 2015; Lv et al., 2017), and even in the human serum and breast milk (Ali et al., 2014; Zhou et al., 2014). Previous researches also revealed that NBFRs have potential neurotoxicity (Jin et al., 2018; Qu et al., 2011), reproductive developmental toxicity (Ma et al., 2018), and endocrine disruption (Johnson et al., 2013; Wang et al., 2019) to aquatic organisms and humans. What's worse, similarity to legacy PBDEs, NBFRs could be accumulated in aquatic organisms and can possibly spread throughout the food chain (Hou et al., 2021; Wu et al., 2020), greatly enhancing the potential risk to the ecosystems and humans.

* Corresponding author.
E-mail address: gaoyp2016@gdut.edu.cn (Y. Gao).

https://doi.org/10.1016/j.watres.2022.118041
Received 10 August 2021; Received in revised form 30 November 2021; Accepted 20 December 2021
Available online 4 January 2022

Generally, UV-induced reductive debromination is the most accepted pathway for PBDEs phototransformation (Davis and Stapleton, 2009; Wei et al., 2013). Similarly, debromination mechanism was also observed in the photochemical transformation of NBFRs (Ling et al., 2019). Besides that, the different ether bond cleavage pathway was proposed in the photochemical transformation of NBFRs (Zhang et al., 2016), suggesting that the degradation mechanism of the legacy and novel brominated flame retardants are controversial. What's more, the previous phototransformation mechanism investigations of NBFRs were proposed only based on the relationship between the molecule structure of substrate and the identified intermediates, which is impossible to clearly determine the main degradation processes, as well as the rate-limiting reaction. More importantly, some more toxic products (e.g. dioxin-like compounds) were formed during the phototransformation of PBDEs (Bendig and Vetter, 2013; Su et al., 2014; 2016). Thus, it is very essential to investigate the transformation mechanism and the toxicity evolution of NBFRs to better understand the environmental behavior, fate and potential risk to aquatic organisms and human health.

Compound specific stable isotope analysis (CSIA) has been confirmed to provide reliable information for determining the reaction pathway (Elsner et al., 2005; Hofstetter and Berg, 2011). It can be not only to distinguish the type of transformation reaction (Aeppli et al., 2012; Birkigt et al., 2015), but also to determine the key step of the reaction (Liu et al., 2020; Peng et al., 2013). Up to now, only a few studies have reported the isotope fractionation in the photodegradation of PBDEs (Ren et al., 2021; Rosenfelder et al., 2011) while the isotope fractionation in NBFRs' phototransformation is still unclear.

In order to probe the environmental transformation characteristic and mechanism of NBFRs, and to better assess their environmental risk, the photochemical transformation of a typical NBFRs (BTBPE) in THF/H_2O under UV irradiation was investigated. Also, its structurally similar PBDE (BDE155) (Fig. S1) under the same conditions was borrowed as a reference. First, the phototransformation kinetics of BTBPE and BDE155 were compared. Then, the photoproducts were identified and employed to deduce its favored structural characteristics. Next, the involved rate-limiting reaction were determined by the stable carbon isotope analysis. At last, phototransformation pathways were tentatively proposed and the potential toxicities of BTBPE as well as its photoproducts were assessed.

2. Material and methods

2.1. Materials

BTBPE (99.9% purity) and BDE155 (99% purity) were purchased from AccuStandard. 2,4,6-Tribromophenol (100 mg L^{-1} in Toluene) and a stock solution of 39 PBDEs (BDE-AAP-A-15X) were also obtained from AccuStandard used as standard for the intermediates. The organic solvents, such as tetrahydrofuran (THF), hexane (HEX), acetonitrile, were HPLC grade and provided by Shanghai ANPEL. Ultrapure water (18.2 MΩ•cm) was obtained from a Milli-Q water purification system.

2.2. Irradiation experiments

For the irradiation experiments, a stock solution of 500 mg L^{-1} of BTBPE in pure THF was prepared. And 3.0 mg L^{-1} of BTBPE was selected for photochemical experiment due to the analysis requirements on mass spectrometry and isotope ratio (shown in Text S1). The photolysis solutions were prepared by evaporating THF in an aliquot of the stock solutions and subsequently re-dissolving in a mixture of THF/H_2O (6/4) solution without adjusting the pH (7.5–7.6). The irradiation experiments were performed with a photochemical reactor (BL-GHX-V, Shanghai Bilon Instrument Co., Ltd., Shanghai, China) equipped with a water-refrigerated 100 W mercury lamp. A water-cooling system was applied to ensure a steady temperature around 27 ± 2 °C. The reaction solution (25 mL) was filled in Pyrex tubes (outer diameter, 20 mm; inner diameter, 16 mm) positioned circularly around the lamp. The Pyrex was used to filter the part of ultraviolet light with wavelengths less than 290 nm (Fang et al., 2008), and the irradiation spectral around the surface of Pyrex tubes is shown in Fig. S2. The dark control experiment was conducted in the same situation but with the tubes wrapped by foil. All the experiments were conducted in at least triplicate.

2.3. Sample pretreatment

500 μL sample were taken from the reaction vessel at fixed intervals and then directly used for HPLC analysis. To identify the photoproducts and measure the stable carbon isotope composition, the Pyrex tube was withdrawn periodically, then, the solution was transferred into a 50 mL teflon centrifuge tube and was adjusted to pH 2–3 by H_2SO_4. After that, the solution was extracted by 3 mL hexane with 3 times. The extracts were combined and dried by Na_2SO_4, then concentrated to near dryness under a gentle nitrogen stream and then dissolved in 100 μL of isooctane for GC–MS analysis and GC-IRMS analysis. The recovery rate of BTBPE and BDE155 were 90.68 ± 3.80% and 94.00 ± 1.94% (mean value ± standard deviation, $n = 15$), respectively.

2.4. Analytical methods

2.4.1. HPLC for concentration analysis

An Agilent 1200 HPLC with diode array detector and a Zorbax SB-C18 column (4.6 × 250 mm, 5-Micron) was employed to quantify the concentration of BTBPE and BDE155. The mobile phase was 100% acetonitrile at a flow rate of 1.2 mL/min and the detection wavelengths for target compounds were 213 nm. The quantification was done with a calibration cure (Fig. S3).

2.4.2. GC–MS for photoproducts analysis

An Agilent GC–MS (7890–5975B) with electron ionization (EI) in full scan mode was adopted for the photoproducts analysis. A DB-5MS column (60 m × 0.25 mm id, 0.25 μm film thickness, J&W Scientific) was used. The oven temperature program for BTBPE was: 70 °C held for 1 min; increased to 280 °C at 10 °C/min and held for 2 min; at last programmed to 300 °C at 20 °C/min and held for 20 min. And the oven temperature program for BDE155 was: 110 °C held for 1 min; increased to 180 °C at 8 °C/min and held for 1 min; followed by an increased to 240 °C at 2 °C/min and held for 5 min; then increased to 280 °C at 2 °C/min and held for 15 min; finally increased to 305 °C at 10 °C/min and held for 10 min. The samples (1 μL) were injected splitless with 1.1 mL/min helium as the carrier gas. The ion fragments m/z scan range was set from 50 to 800.

2.4.3. GC-IRMS for carbon isotope analysis

A Trace GC Ultra-IsoLink Delta V Advantage isotope ratio mass spectrometer (GC-IRMS, Thermo-Fisher Scientific, Waltham, MA, USA) was hired to measure the $\delta^{13}C$ values. The method was borrowed from Huang et al. (2019) but with modifications on GC programs: a DB-5MS column (60 m × 0.25 mm id, 0.25 μm film thickness, J&W Scientific) was used with the following oven temperature program: 70 °C held for 1 min; increased to 280 °C at 10 °C/min and held for 2 min; at last programmed to 300 °C at 20 °C/min and held for 20 min. The samples (1 μL) were injected splitless with 1.1 mL/min helium as the carrier gas, and the combustion interface was maintained at a temperature of 1050 °C. All samples were run at least three times and the deviation is less than 0.5‰. And a standard mixture including 100 mg L^{-1} BTBPE and 100 mg L^{-1} BDE155 was tested begin and after every 3 or 4 samples to verify a constant instrumental condition. More details for this method can be found in Text S2.

2.4.4. Theoretical calculation

Quantum chemical calculation was performed using Gaussian 09 program (Frisch et al., 2009). The geometry of BTBPE was fully

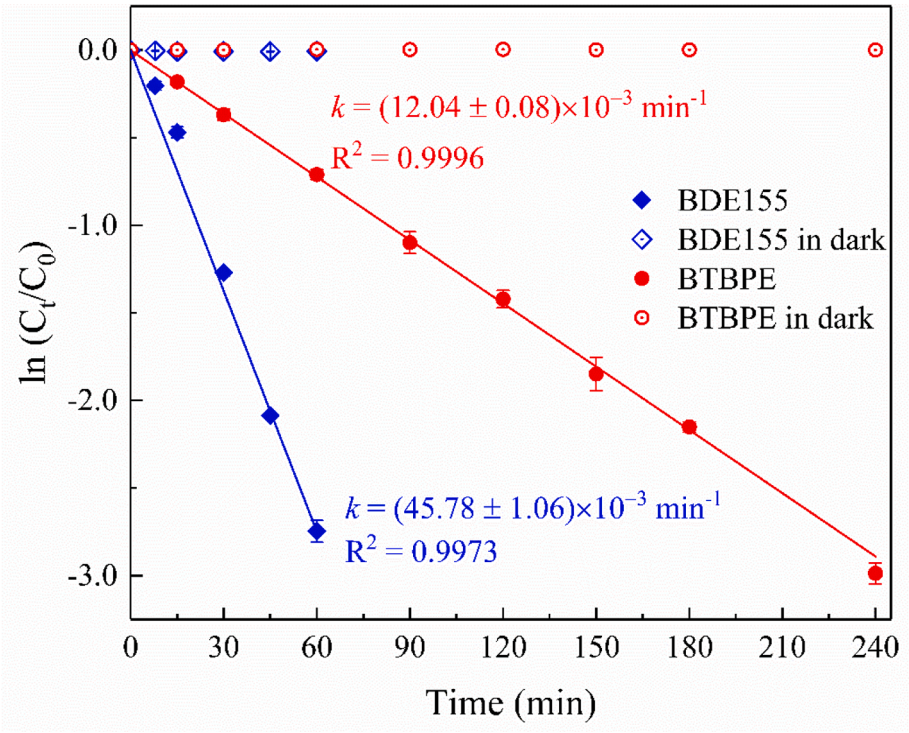

Fig. 1. The phototransformation kinetics of BTBPE and BDE155.

optimized with hybrid density functional theory (DFT) using the M06–2X functional (Walker et al., 2013) and the basis set of 6–31+*G*(d). The adverse effects of BTBPE, BDE155 and their transformation products were assessed using a commercial advanced chemistry development (ACD/Labs Percepta) program (ACD/Labs Percepta, 2016). This tool can provide full complement of physiochemical properties, the absorption, distribution, metabolism, excretion (ADME) and toxicity parameters including health effects. It is proven that this program can successfully estimate the health risk of organic pollutants, e.g. organophosphate flame retardants (Chen et al., 2020), and short-chain chlorinated paraffins (Wang et al., 2021).

2.5. Data and statistical analysis

2.5.1. Kinetic parameters analysis

The phototransformation rate constants was expressed as the k notation, following the pseudo-first-order kinetics (Eq. (1)):

$$\ln\left(\frac{C_t}{C_0}\right) = -kt \tag{1}$$

where C is the concentration of reactant and the subscript t and 0 represent the reaction time is t min and 0 min, respectively, k is obtained based on the linear regression of ln (C_t/C_0) vs time (t) without forcing through zero.

2.5.2. Carbon stable isotope analysis

The stable carbon isotope data was expressed as the δ notation, calculated by the follow equation (Eq. (2)):

$$\delta(\%) = \left(\frac{R_{sample}}{R_{standard}} - 1\right) \times 1000 \tag{2}$$

where R_{sample} and $R_{standard}$ are the ratios of ^{13}C to ^{12}C in samples and the international standard, V-PDB (Vienna Pee Dee Belemnite), respectively.

The carbon isotope enrichment factor was expressed as the ε notation, formulated by the Rayleigh equation (Eq. (3)):

$$\ln\left(\frac{\delta_t + 1}{\delta_0 + 1}\right) = \frac{\varepsilon}{1000}\ln f \tag{3}$$

where *f* represents the fraction of compound remaining and is calculated as the ratio of C_t to C_0, ε is obtained from the slope of the linear regression of $\ln\left(\frac{\delta_t+1}{\delta_0+1}\right)$ vs ln*f* (not forced through zero).

Differences in the reaction rate caused by the presence of isotope was called kinetic isotope effect (KIE), defined by the follow equation (Eq. (4))

$$\mathrm{KIE} = \frac{^{l}k}{^{h}k} \tag{4}$$

where ^{l}k and ^{h}k are the reaction rate constants of the specific bonds which containing a light or heavy isotope, respectively.

If the KIE is not masked by other reaction steps that are less or not isotope sensitive or other kinetic phenomena, its value is approached by the apparent kinetic isotope effect (AKIE) (Hofstetter and Berg, 2011), which considered the intramolecular isotopic competition during the rate-determining step of a specific reaction, and was formulated by the follow equation (Eq. (5)):

$$\mathrm{AKIE} = \left(\frac{^{l}k}{^{h}k}\right)_{apparent} = \frac{1}{1 + n \times \frac{z}{x} \times \varepsilon} \tag{5}$$

where n is the number of carbon atoms in the molecule, x is the number of carbon atoms at reactive sites, z is the number of carbon atoms in identical reaction positions undergoing intramolecular competition. Here, for both BTBPE and BDE155, x = z because of their symmetrical molecular structure.

3. Results and discussion

3.1. Photodegradation kinetics

Fig. 1 portrays the phototransformation kinetics of the

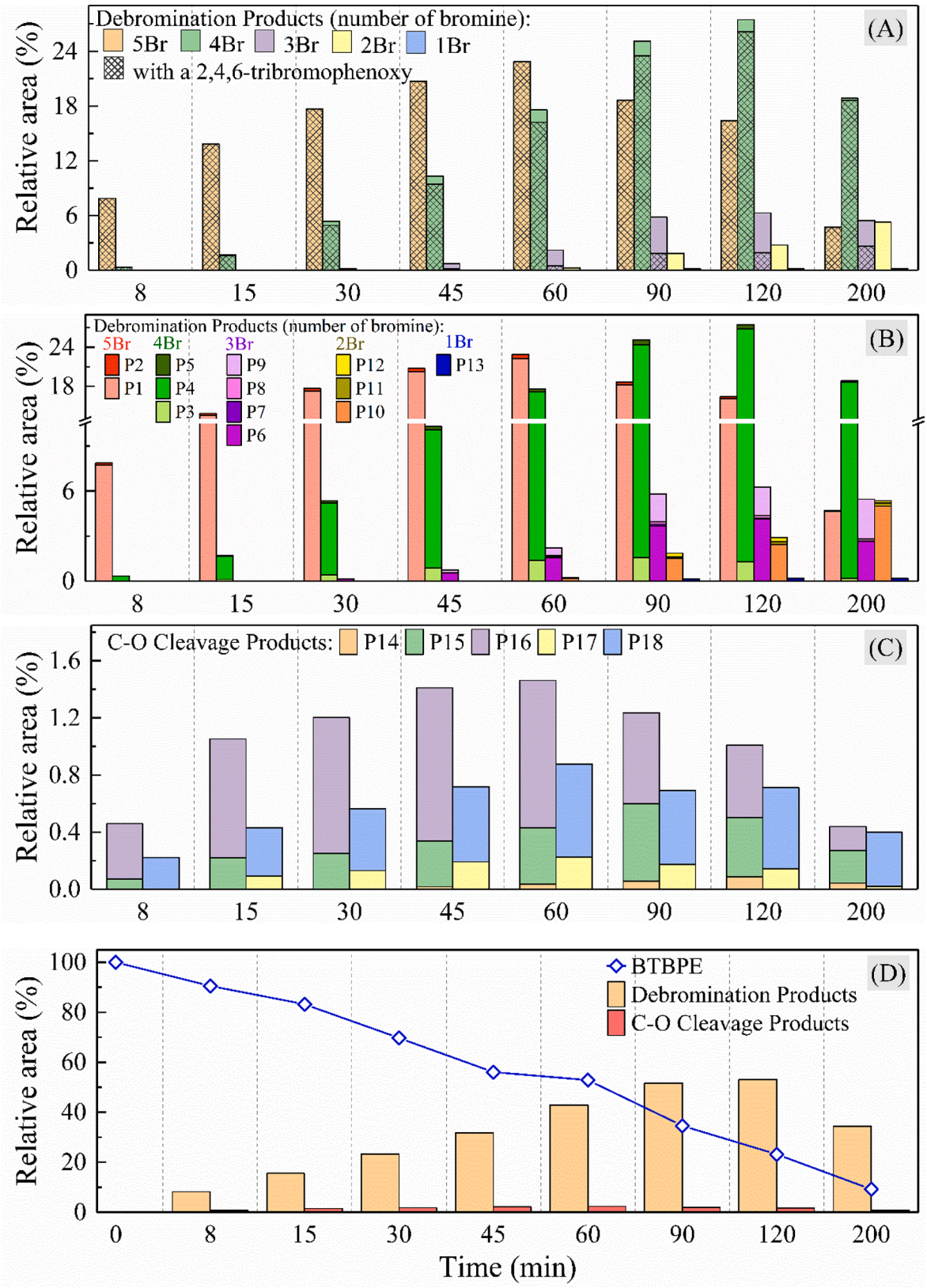

Fig. 2. Evolution profiles of the identified products of BTBPE. (A–B): debromination products; (C): C—O cleavage products; (D): the comparison of debromination products and C—O cleavage products. (Relative areas were calculated with the area of BTBPE at 0 min as the reference).

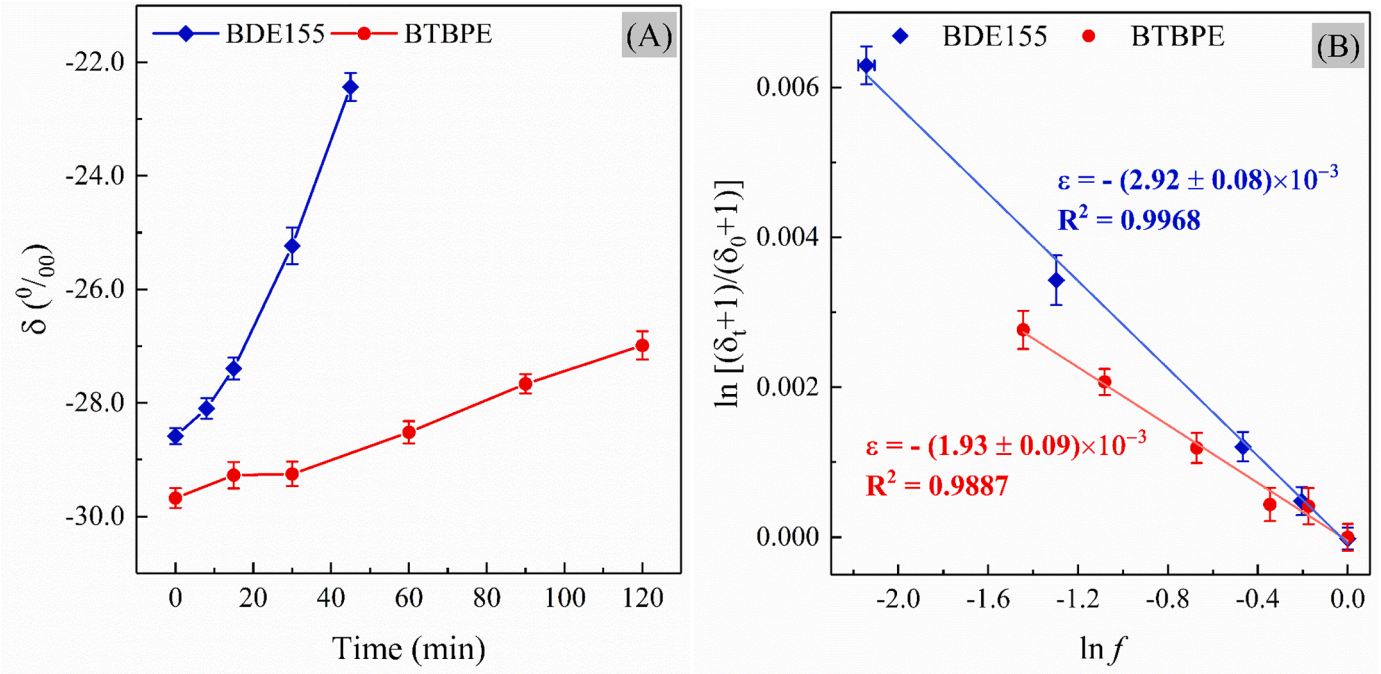

Fig. 3. Stable carbon isotope fractionation of BTBPE and BDE155 during photolysis. (A) changes of isotope ratio with time. (B) Rayleigh plots during the photodegradation.

representatives of NBFRs (BTBPE) and legacy BFRs (BDE155). No significant degradation for the two BFRs was observed in the dark control. However, upon UV irradiation, the concentration of both BTBPE and BDE155 declined rapidly, and followed a pseudo-first-order kinetics model ($R^2 > 0.997$). The phototransformation rate constants (k) for BTBPE was obtained as (12.04 ± 0.08) × 10^{-3} min^{-1}, nearly 4 times lower than that of BDE155, (44.69 ± 1.12) × 10^{-3} min^{-1}. These differences may be contributed to their absorbance behavior since the irradiation spectrum and absorption spectra of BTBPE overlap is less than those of BDE155 (Fig. S2 and Text S3). Previous studies have shown that the wider overlap, the faster photodegradation rate (Eriksson et al., 2004; Wei et al., 2013). Thus, compared to the legacy BFRs (BDE155), the novel NBFRs (BTBPE) may be less photo-chemically reactive, potentially causing more persistent in environment.

3.2. Transformation products

3.2.1. Transformation products and debromination model of BDE155

In order to better identify the phototransformation products of BTBPE, the identification of products was firstly performed on BDE155 with the structural similarity, by comparison with the standard solution of 39 PBDEs (BDE-AAP-A-15X). Only 9 debrominated photoproducts were identified and confirmed by their standards in the GC–MS chromatogram (Fig. S4), including BDE100, 75, 47, 32, 28, 17, 15, 8 and 3, with structures summarized in Table S4. Interestingly, no bromophenols were detected, indicating that fission of ether bonds seems unlikely to occur under the experimental conditions.

With the increase of irradiation time, the less-brominated congeners gradually appeared, especially the para bromine fraction gradually increased (Fig. S5A). This suggests that ortho debromination is the dominant mechanism for BDE155 transformation, in agreement with the previous studies (Davis and Stapleton, 2009; Eljarrat et al., 2011; Shih and Wang, 2009; Wei et al., 2013). More interestingly, the debromination occurred preferentially in the phenyl ring without a 2,4,6-tribromo substitution model because the proportion of these products with a 2,4,6-tribromophenoxy is significantly larger in high brominated products (>3Br) (Fig. S5A). This is contrary to the most accepted rule of stepwise reductive debromination of PBDEs, which believes that debromination usually occurs in the more highly brominated phenyl ring, especially a fully substituted one (Wei et al., 2013). Possible explanation is that the two phenyl rings are relatively independent (Saeed et al., 2020), and the 2,4,6-tribromophenoxy is more stable than other bromophenoxys. This conjecture is confirmed by the results observed by Fang et al. (2008), that is, the photochemical degradation rate of BDE100 (24–246) is much slower than that of BDE99 (24–245), and the major product of BDE100 (24–246) was BDE75 (4–246) instead of BDE47 (24–24).

3.2.2. Transformation products of BTBPE

Totally 18 photoproducts were identified in the GC–MS chromatogram (Fig. S7), and their structures (listed in Table S5) were identified by their mass spectra (Fig. S8) with the analysis discussed in Text S4. Besides 13 debromination photoproducts (P1-P13), it was also noticed three C—O cleavage products (P14, P15 (tribromophenol, TBP), and P16) and two of their derived debrominated products (P17 and P18 (dibromophenol, DBP). This is similar with the observation in pure organic solvent (Zhang et al., 2016), but the photoproducts formed by the cleavage of the phenoxy bond (C_4—O_3, Fig. S1) has not been detected, indicating that the phenoxy bond seems unlikely to break under our experimental conditions. Further, the theoretical calculation shows the bond length (1.36 Å) of C_4—O_3 is shorter than that of C_2—O_3 (1.43 Å) (Fig. S9), confirming the cleavage of phenoxy bond is more difficult.

Seen from the whole evolutions of the debromination products (Fig. 2A), BTBPE is debrominated stepwise, and tends to keep a 2,4,6-tribromophenoxy unchanged since the products with this structure (e.g. P1, P2, P4, P5 and P9) have a relative larger peak area. By analyzing the isomers in the debromination products (Fig. 2B), the dominated tetrabromo-products is P4, formed by removing an ortho bromine atom from the 2,4-dibromophenyl, and the secondary tribromo-products is P9, formed by removing a para bromine atom from the 4-monobromophenoxy, instead of the 2,4,6-tribromophenoxy. Therefore, we concluded that the ortho bromine atoms are more vulnerable than the para bromine atoms and the 2,4,6-tribromophenoxy is more stable than 2,4-dibromophenoxy and 4-monobromophenoxy.

As for the five C—O cleavage products, two channels to break the ether bond were proposed: One is the direct fission of C_2—O_3 to form photoproducts (P14 and P15) and the other is the 1,3-hydeogen shift

Table. 1
Spectral absorption data, phototransformation rate constants (k), half-life ($t_{1/2}$), $\delta^{13}C$ and ε for BTBPE and BDE155.s.

	Spectral absorption data		k ($\times10^{-3}$ min^{-1})	Half-life (min)	$\delta^{13}C0$ (‰)	$\delta^{13}Ct$ (‰)	$\delta^{13}Cd$ (‰)	ε (‰)	AKIE
	λ_{max} (nm)	Molar absorptivity (L mol^{-1} cm^{-1})							
BTBPE	290	917	12.04 ± 0.08	57.57	−29.68 ± 0.17	−26.99 ± 0.25	−29.44 ± 0.29	−1.93 ± 0.09	1.028
BDE155	295	1931	44.69 ± 1.12	15.51	−28.58 ± 0.14	−22.43 ± 0.24	−28.66 ± 0.12	−2.92 ± 0.08	1.036

$\delta^{13}C_0$: the value of $\delta^{13}C$ at time $t = 0$ min.
$\delta^{13}C_t$: the value of $\delta^{13}C$ at time $t = 120$ min for BTBPE and $t = 45$ min for BDE155.
$\delta^{13}C_d$: the value of $\delta^{13}C$ at time $t = 200$ min for the dark control.

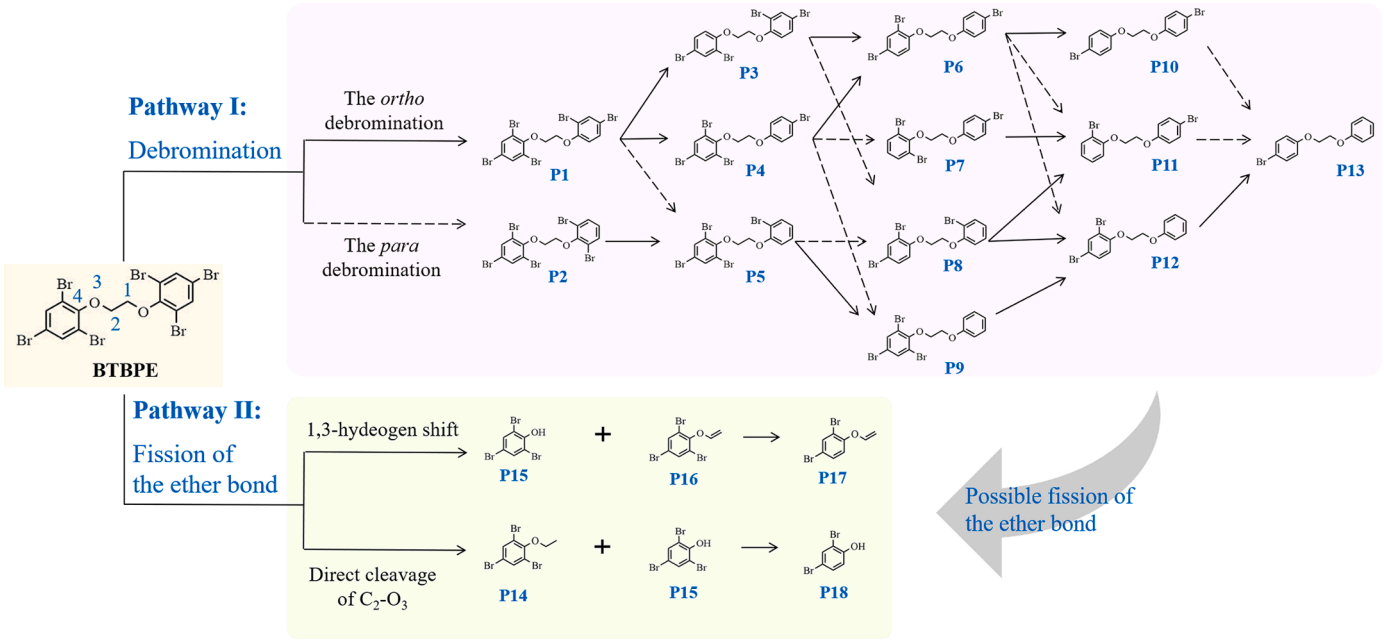

Fig. 4. Proposed phototransformation pathways of BTBPE. In pathway I, the solid arrow means the ortho debromination, while the dashed arrow is the para debromination.

from C_1 to the flanked O_3 atom to form photoproducts (P15 and P16). The details for the process are discussed in Text S4. Furthermore, the relative area of P16 is much larger than that of P14 (Fig. 2C), indicating the 1,3-hydeogen shift is the main channel to break the ether bond. Comparing to the debromination products, the yield of the C—O cleavage products is less (Fig. 2D). This result may be due to the faster photodegradation rate of these tribromophenol analogs (Zhao et al., 2017). Nevertheless, it is not clear whether the ether bond cleavage is an important pathway through the analysis of the photoproducts, and this should be further discussed.

3.3. Compound specific stable isotope analysis

The evolution profiles of carbon isotope ratios for BTBPE and BDE155 during phototransformation are shown in Fig. 3A. After phototransformation, both BTBPE and BDE155 have a degree of ^{13}C enrichment while no significant carbon isotope fraction was observed in the dark control (Table. 1). The significant carbon isotope fractionation can be quantified by the Rayleigh equation (Eq. (3)) (Fig. 3B), and the corresponding isotope enrichment factors ε were obtained as −1.93 ± 0.09‰ for BTBPE and −2.92 ± 0.08‰ for BDE155. In order to elucidate the phototransformation mechanisms, the apparent kinetic isotope effect (AKIE) was further derived (Eq. (5)) (Table. 1). The AKIE for BDE155 (1.036) was very close to the theoretical carbon kinetic isotope effect (KIE) calculated for C-Br bond cleavage (1.040, Table S3), meaning that the cleavage of C-Br bond is the rate-limiting reaction for BDE155 phototransformation (Elsner et al., 2005; Hofstetter and Berg, 2011). This result is consistent with the above-mentioned analysis that stepwise debromination is the main photodegradation pathway of BDE155. However, the AKIE of BTBPE (1.028) seems to difficultly determine one rate-limiting reaction for BTBPE photo-transformation. That is, if the cleavage of C—H bond is the only rate-limiting reaction in BTBPE phototransformation, the AKIE should close to 1.021 (Table S3); otherwise, 1.040 for the cleavage of C-Br bond only. In fact, the observed AKIE of BTBPE (1.028) is between the theoretical KIE of C—H bond cleavage (1.021) and C-Br bond cleavage (1.040), indicating that the two reaction pathways could occur simultaneously. Namely, both C-Br bond cleavage and C—H bond cleavage are the significant rate-limiting reactions for BTBPE, and more details are discussed in Text S7.

3.4. Phototransformation pathways

Based on the photoproducts analysis and CSIA analysis, the phototransformation pathways of BTBPE and BDE155 were tentatively proposed and shown in Fig. 4 and Fig. S6, respectively. A successive losses of bromine atoms was observed during the phototransformation of BDE155 (Fig. S5A), in agreement with previous studies (Fang et al., 2008; Shih and Wang, 2009). Thus, debromination is the dominant mechanism for BDE155 phototransformation, resulting in formation of less brominated congeners. Whereas, BTBPE undergoes two pathways: One is the stepwise debromination to form a series of lower brominated products (P1-P13, Pathway I in Fig. 4) and the other is the fission of the ether bond to form three tribromophenol homologue along with their

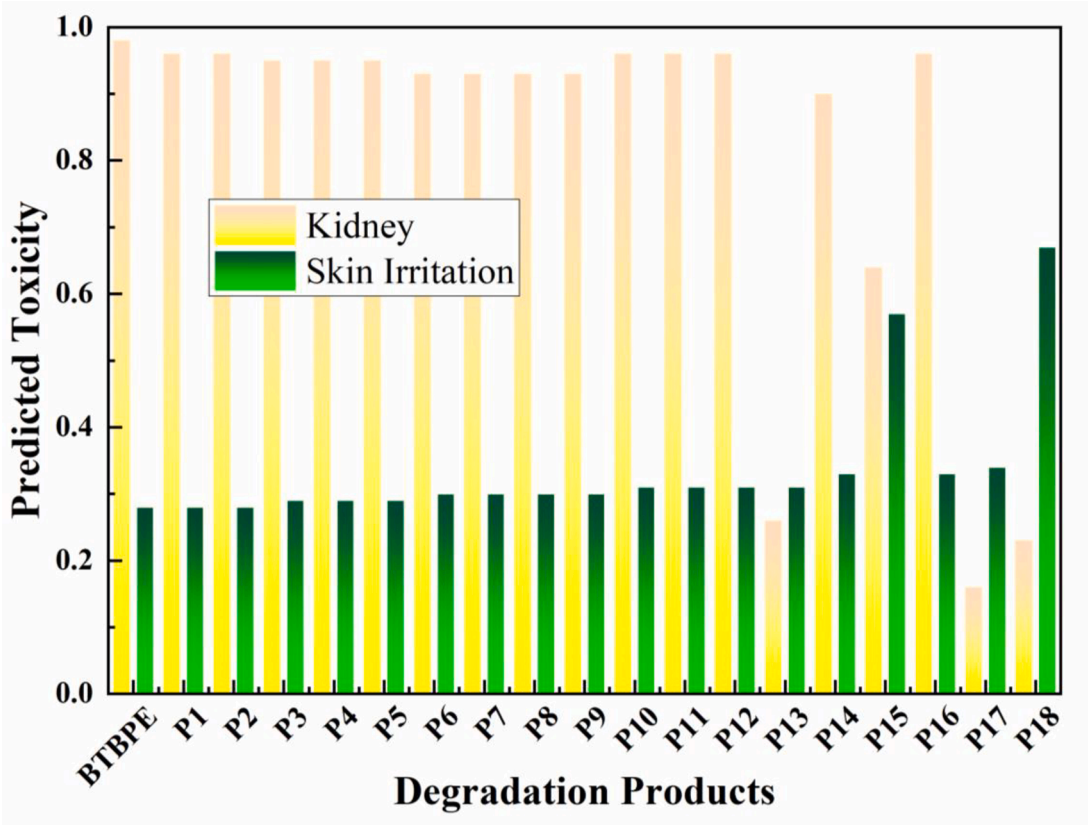

Fig. 5. Predicted toxicity of BTBPE and its phototransformation products.

debrominated derivatives (P14-P18, Pathway II in Fig. 4). The products (P1, P3, P4, P6, P14-P18) were also observed in BTBPE phototransformation under pure organic solvents (Zhang et al., 2016). Moreover, by compound-specific stable isotope analysis, the rate-limiting reactions for BTBPE were determined as the cleavage of C-Br bond accompanied with the breaking of C_1—H bond, which is the rate-limiting step of the 1,3-hydeogen shift (Altarawneh and Dlugogorski, 2014).

3.5. Toxicity assessments

Since the original pollutants (BTBPE and BDE155) have adverse effects on kidney system (Zhao et al., 2020) and potential health risks via dermal absorption (Cao et al., 2019), the potential toxicity of degradation products is necessary to be investigated. The probability (p) of adverse effect on kidney system and skin irritation were tentatively assessed using ACD/Labs Percepta software (ACD/Labs Percepta, 2016), which is confirmed in the application of environmental chemistry, e.g. organophosphate flame retardants (Chen et al., 2020) and short-chain chlorinated paraffins (Wang et al., 2021). The obtained results were displayed in Figs. 5 and S10. Herein, p is between 0 and 1, and the greater the p value is, the stronger the adverse effects would impose. Both BTBPE and BDE155 with p of 0.98 and 0.97, respectively, have toxicity on kidney, confirmed by the previous research that the effects of PBDEs on kidney injury (Zhao et al., 2020). And the stepwise debromination is a promising detoxification pathway because the debromination products were less toxic than the parent. Unlike BDE155, the nephrotoxicity of the dibromo-products is slightly increased than that of the tribromo-products, indicating that the nephrotoxicity of debrominated products of BTBPE does not always decrease with the decreasing number of bromines. To our best knowledge, the mechanism of toxicity difference is still unclear and further study is needed. Meantime, a significant toxicity increase in skin irritation was found for the C—O cleavage products of BTBPE (Fig. 5), implying that BTBPE can be degraded to the more toxic products, especially the bromophenols (P15, P18). In addition to the increased skin irritation, bromophenols has also been confirmed to have neurotoxicity (Lyubimov et al., 1998), and endocrine disrupting effects (Olsen et al., 2002), and even can be transformed to the more toxic brominated dioxins (Arnoldsson et al., 2012).

4. Conclusion

Our study demonstrates the novel BTBPE can be degraded under UV irradiation, and its rate constants is four times lower than that of legacy BDE155, indicating that the stronger environmental persistence of novel BTBPE. Compared to the only debromination of BDE155, the potential multiple pathways via debromination and the ether bond cleavage were observed in the phototransformation of BTBPE using comprehensive photoproducts identification and compound-specific stable isotope analysis. Furthermore, the computational toxicity data show that BTBPE can transform into the more toxic products. Especially the bromophenols (P15, P18) were produced from the ether bond cleavage pathway, greatly enhancing its environmental risk. In a word, the phototransformation of NBFRs should be paid great attention, in particular the formation of the more toxic products.

Declaration of Competing Interest

The authors declare that they have no known competing financial interests or personal relationships that could have appeared to influence the work reported in this paper.

Acknowledgments

The authors appreciate the financial supports from National Natural

Science Foundation of China (41977365, 41425015 and 41773129), National Key Research and Development Program of China (2019YFC1804501, 2019YFC1804502), Local Innovative and Research Teams Project of Guangdong Pearl River Talents Program (2017BT01Z032 and 2017BT01Z134), and Strategic Priority Research Program of Chinese Academy of Science (XDPB2001).

Supplementary materials

Supplementary material associated with this article can be found, in the online version, at doi:10.1016/j.watres.2022.118041.

References

ACD/Labs Percepta, 2016. Advanced Chemistry Development Inc., Toronto, ON, Canada.
Aeppli, C., Tysklind, M., Holmstrand, H., Gustafsson, Ö., 2012. Use of Cl and C isotopic fractionation to identify degradation and sources of polychlorinated phenols: mechanistic study and field application. Environ. Sci. Technol. 47 (2), 790–797.
Ali, N., Mehdi, T., Malik, R.N., Eqani, S.A.M.A.S., Kamal, A., Dirtu, A.C., Neels, H., Covaci, A., 2014. Levels and profile of several classes of organic contaminants in matched indoor dust and serum samples from occupational settings of Pakistan. Environ. Pollut. 193, 269–276.
Altarawneh, M., Dlugogorski, B.Z., 2014. Thermal decomposition of 1,2-bis(2,4,6-tribromophenoxy)ethane (BTBPE), a novel brominated flame retardant. Environ. Sci. Technol. 48 (24), 14335–14343.
Arnoldsson, K., Andersson, P.L., Haglund, P., 2012. Formation of environmentally relevant brominated dioxins from 2,4,6,-tribromophenol via bromoperoxidase-catalyzed dimerization. Environ. Sci. Technol. 46 (13), 7239–7244.
Bendig, P., Vetter, W., 2013. UV-induced formation of bromophenols from polybrominated diphenyl ethers. Environ. Sci. Technol. 47 (8), 3665–3670.
Birkigt, J., Gilevska, T., Ricken, B., Richnow, H.H., Vione, D., Corvini, P.F.X., Nijenhuis, I., Cichocka, D., 2015. Carbon stable isotope fractionation of sulfamethoxazole during biodegradation by microbacteriumsp. Strain BR1 and upon direct photolysis. Environ. Sci. Technol. 49 (10), 6029–6036.
Cao, Z., Chen, Q., Zhu, C., Chen, X., Wang, N., Zou, W., Zhang, X., Zhu, G., Li, J., Mai, B., Luo, X., 2019. Halogenated organic pollutant residuals in human bared and clothing-covered skin areas: source differentiation and comprehensive health risk assessment. Environ. Sci. Technol. 53 (24), 14700–14708.
Chen, M., Liao, X.L., Yan, S.C., Gao, Y.P., Yang, C., Song, Y.Y., Liu, Y., Li, W.Q., Tsang, S. Y., Chen, Z.F., Qi, Z.H., Cai, Z.W., 2020. Uptake, accumulation, and biomarkers of PM(2.5)-associated organophosphate flame retardants in C57BL/6 mice after chronic exposure at real environmental concentrations. Environ. Sci. Technol. 54 (15), 9519–9528.
Davis, E.F., Stapleton, H.M., 2009. Photodegradation pathways of nonabrominated diphenyl ethers, 2-ethylhexyltetrabromobenzoate and Di(2-ethylhexyl) tetrabromophthalate: identifying potential markers of photodegradation. Environ. Sci. Technol. 43 (15), 5739–5746.
Eljarrat, E., Feo, M.L., Barceló, D., Eljarrat, E., Barceló, D., 2011. Brominated Flame Retardants. Springer Berlin Heidelberg. Heidelberg, Berlin, pp. 187–202.
Elsner, M., Zwank, L., Hunkeler, D., Schwarzenbach, R.P., 2005. A new concept linking observable stable isotope fractionation to transformation pathways of organic pollutants. Environ. Sci. Technol. 39 (18), 6896–6916.
Eriksson, J., Green, N., Marsh, G., Bergman, A., 2004. Photochemical decomposition of 15 polybrominated diphenyl ether congeners in methanol/water. Environ. Sci. Technol. 38 (11), 3119–3125.
Fang, L., Huang, J., Yu, G., Wang, L., 2008. Photochemical degradation of six polybrominated diphenyl ether congeners under ultraviolet irradiation in hexane. Chemosphere 71 (2), 258–267.
Frisch, M.J., Trucks, G.W., Schlegel, H.B., Scuseria, G.E., Robb, M.A., Cheeseman, J.R., Scalmani, G., Barone, V., Mennucci, B., Petersson, G.A., Nakatsuji, H., Caricato, M., Li, X., Hratchian, H.P., Izmaylov, A.F., Bloino, J., Zheng, G., Sonnenberg, J.L., Hada, M., Ehara, M., Toyota, K., Fukuda, R., Hasegawa, J., Ishida, M., Nakajima, T., Honda, Y., Kitao, O., Nakai, H., Vreven, T., Montgomery Jr., J.A., Peralta, J.E., Ogliaro, F., Bearpark, M.J., Heyd, J., Brothers, E.N., Kudin, K.N., Staroverov, V.N., Kobayashi, R., Normand, J., Raghavachari, K., Rendell, A.P., Burant, J.C., Iyengar, S. S., Tomasi, J., Cossi, M., Rega, N., Millam, N.J., Klene, M., Knox, J.E., Cross, J.B., Bakken, V., Adamo, C., Jaramillo, J., Gomperts, R., Stratmann, R.E., Yazyev, O., Austin, A.J., Cammi, R., Pomelli, C., Ochterski, J.W., Martin, R.L., Morokuma, K., Zakrzewski, V.G., Voth, G.A., Salvador, P., Dannenberg, J.J., Dapprich, S., Daniels, A.D., Farkas, Ö., Foresman, J.B., Ortiz, J.V., Cioslowski, J., Fox, D.J., 2009. Gaussian 09. Gaussian, Inc., Wallingford, CT, USA.
Hofstetter, T.B., Berg, M., 2011. Assessing transformation processes of organic contaminants by compound-specific stable isotope analysis. TrAC Trends Anal. Chem. 30 (4), 618–627.
Hou, R., Lin, L., Li, H., Liu, S., Xu, X., Xu, Y., Jin, X., Yuan, Y., Wang, Z., 2021. Occurrence, bioaccumulation, fate, and risk assessment of novel brominated flame retardants (NBFRs) in aquatic environments — a critical review. Water Res. 198, 117168.
Huang, C., Zeng, Y., Luo, X., Ren, Z., Tang, B., Lu, Q., Gao, S., Wang, S., Mai, B., 2019. *In situ* microbial degradation of PBDEs in sediments from an E-waste site as revealed by positive matrix factorization and compound-specific stable carbon isotope analysis. Environ. Sci. Technol. 53 (4), 1928–1936.
Jin, M.Q., Zhang, D., Zhang, Y., Zhou, S.S., Lu, X.T., Zhao, H.T., 2018. Neurological responses of embryo-larval zebrafish to short-term sediment exposure to decabromodiphenylethane. J. Zhejiang Univ. Sci. B 19 (5), 400–408.
Johnson, P.I., Stapleton, H.M., Mukherjee, B., Hauser, R., Meeker, J.D., 2013. Associations between brominated flame retardants in house dust and hormone levels in men. Sci. Total Environ. 445-446, 177–184.
Kolic, T.M., Shen, L., MacPherson, K., Fayez, L., Gobran, T., Heim, P.A., Marvin, C.H., Arsenault, G., Reiner, E.J., 2009. The analysis of halogenated flame retardants by GC-HRMS in environmental samples. J. Chromatogr. Sci. 47 (1), 83–91.
Li, P., Wu, H., Li, Q., Jin, J., Wang, Y., 2015. Brominated flame retardants in food and environmental samples from a production area in China: concentrations and human exposure assessment. Environ. Monit. Assess. 187 (11), 719.
Ling, S., Huang, K., Tariq, M., Wang, Y., Chen, X., Zhang, W., Lin, K., Zhou, B., 2019. Photodegradation of novel brominated flame retardants (NBFRs) in a liquid system: kinetics and photoproducts. Chem. Eng. J. 362, 938–946.
Liu, Y., Mekic, M., Carena, L., Vione, D., Gligorovski, S., Zhang, G., Jin, B., 2020. Tracking photodegradation products and bond-cleavage reaction pathways of triclosan using ultra-high resolution mass spectrometry and stable carbon isotope analysis. Environ. Pollut. 264, 114673.
Lv, S., Niu, Y., Zhang, J., Shao, B., Du, Z., 2017. Atmospheric pressure chemical ionization gas chromatography mass spectrometry for the analysis of selected emerging brominated flame retardants in foods. Sci. Rep. 7, 43998.
Lyubimov, A.V., Babin, V.V., Kartashov, A.I., 1998. Developmental neurotoxicity and immunotoxicity of 2,4,6-tribromophenol in Wistar rats. Neurotoxicology 19 (2), 303–312.
Ma, Y., Venier, M., Hites, R.A., 2012. Tribromophenoxy flame retardants in the Great Lakes atmosphere. Environ. Sci. Technol. 46 (24), 13112–13117.
Ma, Z., Peng, H., Jin, Y., Zhang, X., Xie, X., Jian, K., Liu, H., Su, G., Tang, S., Yu, H., 2018. Multigenerational Effects and Demographic Responses of Zebrafish (Danio rerio) Exposed to Organo-Bromine Compounds. Environ. Sci. Technol. 52 (15), 8764–8773.
Olsen, C.M., Meussen-Elholm, E.T.M., Holme, J.A., Hongslo, J.K., 2002. Brominated phenols: characterization of estrogen-like activity in the human breast cancer cell-line MCF-7. Toxicol. Lett. 129 (1–2), 55–63.
Peng, X., Feng, L., Li, X., 2013. Pathway of diethyl phthalate photolysis in sea-water determined by gas chromatography–mass spectrometry and compound-specific isotope analysis. Chemosphere 90 (2), 220–226.
Qu, G., Shi, J., Wang, T., Fu, J., Li, Z., Wang, P., Ruan, T., Jiang, G., 2011. Identification of tetrabromobisphenol A diallyl ether as an emerging neurotoxicant in environmental samples by bioassay-directed fractionation and HPLC-APCI-MS/MS. Environ. Sci. Technol. 45 (11), 5009–5016.
Ren, Z., Zeng, Y., Luo, X., Huang, C., Tian, Y., Gao, S., Mai, B., 2021. Observable carbon isotope fractionation in the photodegradation of polybrominated diphenyl ethers by simulated sunlight. Chemosphere 266, 128950.
Renner, R., 2004. In US., flame retardants will be voluntarily phased out. Environ. Sci. Technol. 38 (1), 14A–15A.
Rosenfelder, N., Bendig, P., Vetter, W., 2011. Stable carbon isotope analysis (delta13C values) of polybrominated diphenyl ethers and their UV-transformation products. Environ. Pollut. 159 (10), 2706–2712.
Saeed, A., Altarawneh, M., Siddique, K., Conesa, J.A., Ortuno, N., Dlugogorski, B.Z., 2020. Photodecomposition properties of brominated flame retardants (BFRs). Ecotoxicol. Environ. Saf. 192 (1), 110272.
Shi, T., Chen, S.J., Luo, X.J., Zhang, X.L., Tang, C.M., Luo, Y., Ma, Y.J., Wu, J.P., Peng, X. Z., Mai, B.X., 2009. Occurrence of brominated flame retardants other than polybrominated diphenyl ethers in environmental and biota samples from southern China. Chemosphere 74 (7), 910–916.
Shih, Y.H., Wang, C.K., 2009. Photolytic degradation of polybromodiphenyl ethers under UV-lamp and solar irradiations. J. Hazard. Mater. 165 (1–3), 34–38.
Su, G., Letcher, R.J., Crump, D., Farmahin, R., Giesy, J.P., Kennedy, S.W., 2014. Photolytic degradation products of two highly brominated flame retardants cause cytotoxicity and mRNA expression alterations in chicken embryonic hepatocytes. Environ. Sci. Technol. 48 (20), 12039–12046.
Su, G., Letcher, R.J., Crump, D., Farmahin, R., Giesy, J.P., Kennedy, S.W., 2016. Sunlight irradiation of highly brominated polyphenyl ethers generates polybenzofuran products that alter dioxin-responsive mRNA expression in chicken hepatocytes. Environ. Sci. Technol. 50 (5), 2318–2327.
Tang, H.P.O., 2013. Recent development in analysis of persistent organic pollutants under the Stockholm convention. TrAC Trends Anal. Chem. 45, 48–66.
Verreault, J., Gebbink, W.A., Gauthier, L.T., Gabrielsen, G.W., Letcher, R.J., 2007. Brominated flame retardants in glaucous gulls from the Norwegian Arctic: more than just an issue of polybrominated diphenyl ethers. Environ. Sci. Technol. 41 (14), 4925–4931.
Walker, M., Harvey, A.J.A., Sen, A., Dessent, C.E.H., 2013. Performance of M06, M06-2X, and M06-HF density functionals for conformationally flexible anionic clusters: M06 functionals perform better than B3LYP for a model system with dispersion and ionic hydrogen-bonding interactions. J. Phys. Chem. A 117 (47), 12590–12600.
Wang, H., Liu, S., Zhang, C., Wan, Y., Chang, H., 2020. Occurrence and mass balance of emerging brominated flame retardants in a municipal wastewater treatment plant. Water Res. 185, 116298.
Wang, M., Gao, Y., Li, G., An, T., 2021. Increased adverse effects during metabolic transformation of short-chain chlorinated paraffins by cytochrome P450: a theoretical insight into 1-chlorodecane. J. Hazard. Mater. 407, 124391.
Wang, X., Ling, S., Guan, K., Luo, X., Chen, L., Han, J., Zhang, W., Mai, B., Zhou, B., 2019. Bioconcentration, biotransformation, and thyroid endocrine disruption of decabromodiphenyl ethane (Dbdpe), a novel brominated flame retardant, in Zebrafish Larvae. Environ. Sci. Technol. 53 (14), 8437–8446.

Wei, H., Zou, Y., Li, A., Christensen, E.R., Rockne, K.J., 2013. Photolytic debromination pathway of polybrominated diphenyl ethers in hexane by sunlight. Environ. Pollut. 174, 194–200.
Wu, J.P., Wu, S.K., Tao, L., She, Y.Z., Chen, X.Y., Feng, W.L., Zeng, Y.H., Luo, X.J., Mai, B.X., 2020. Bioaccumulation characteristics of PBDEs and alternative brominated flame retardants in a wild frog-eating snake. Environ. Pollut. 258, 8.
Zhang, H., Bayen, S., Kelly, B.C., 2015. Multi-residue analysis of legacy POPs and emerging organic contaminants in Singapore's coastal waters using gas chromatography-triple quadrupole tandem mass spectrometry. Sci. Total Environ. 523, 219–232.
Zhang, Y.N., Chen, J., Xie, Q., Li, Y., Zhou, C., 2016. Photochemical transformation of five novel brominated flame retardants: kinetics and photoproducts. Chemosphere 150, 453–460.
Zhao, H.X., Jiang, J.Q., Wang, Y.L., Xie, Q., Qu, B.C., 2017. Phototransformation of 2,4,6-tribromophenol in aqueous solution: kinetics and photolysis products. J. Environ. Sci. Health Part A 52 (1), 45–54. -Toxic/Hazardous Substances & Environmental Engineering.
Zhao, X., Chen, T., Wang, D., Du, Y., Wang, Y., Zhu, W., Bekir, M., Yu, D., Shi, Z., 2020. Polybrominated diphenyl ethers and decabromodiphenyl ethane in paired hair/serum and nail/serum from corresponding chemical manufacturing workers and their correlations to thyroid hormones, liver and kidney injury markers. Sci. Total Environ. 729, 139049.
Zhou, S.N., Buchar, A., Siddique, S., Takser, L., Abdelouahab, N., Zhu, J., 2014. Measurements of selected brominated flame retardants in nursing women: implications for human exposure. Environ. Sci. Technol. 48 (15), 8873–8880.